Synthesis and Characterisation of Controllably Functionalised Polyaniline Nanofibres

Emer Lahiff,[a*] Trevor Woods[b], Werner Blau[b], Gordon G. Wallace[c] and Dermot Diamond[a]

[a] *Adaptive Sensors Group, National Centre for Sensor Research, Dublin City University, Dublin 9, Ireland.*
[b] *Molecular Electronics and Nanotechnology Group, School of Physics, Trinity College, Dublin 2, Ireland.*
[c] *ARC Centre for Nanostructured Electromaterials, Intelligent Polymer Research Institute, University of Wollongong, Wollongong, NSW 2522, Australia.*

**Corresponding Author: Tel: 353-1-7007926; Fax: 353-1-700;*
E-mail address: emer.lahiff@dcu.ie

Received XXX, Accepted XXX

Abstract

A novel method for functionalising solution based polyaniline (PAni) nanofibres is reported whereby the degree of side-chain attachment can be controllably altered. The covalent attachment of functional side-groups to the surface of PAni nanostructures is achieved by post-polymerisation reflux in the presence of a nucleophile and the functionalised nanomaterial can be purified by simple centrifugation. The technique is therefore easily scalable. We demonstrate that control over the extent of side-chain attachment can be achieved simply by altering the amount of nucleophile added during reflux. We provide evidence that covalently attached carboxlate side-chains influence the doping mechanism of polyaniline and can be used to introduce self-doping behaviour. Acid functionalised nanofibres remain redox active and retain their optical switching capabilities in response to changes in the local chemical environment, thus making them suitable for adaptive sensing applications.

Keywords: Conducting polymers, nanofibres, functionalisation, facile synthesis, self-doping

1. Introduction

Recent advances in the design and synthesis of one-dimensional nanomaterials, including organic and inorganic nanowires, have attracted much attention[1-5]. However, it remains a challenge to efficiently and controllably attach functional side-groups to these materials. The attachment of functional groups can be used to tailor the interactions of nanomaterials with their environment[6, 7]. In particular, the attachment of side-groups to inherently conducting polymer (ICP) nanostructures means that functionalities are anchored to a redox active low dimensional organic conductor. Where acid functional groups are attached the conducting polymer can become self-doping, thus reducing the need for external dopants and hence improving stability.[8, 9]

Researchers and industrialist have studied ICPs with a view to exploiting their properties for applications such as electronic devices, sensors and actuators[10-12]. Polyaniline (PAni) is an example of a stable ICP and can be classified as an 'adaptive material' in that it can be switched between two or more forms (each with their own distinct characteristics) using an external stimulus[13]. In contrast to a classical metallic conductor or a polymeric insulator, PAni can be switched reversibly between an insulating emeraldine base form and a conducting emeraldine salt[14]. More recently, interest has developed in the area of nanostructured polyaniline[15-20]. These one-dimensional objects combine the advantages of an organic conductor and a high surface area material, thus making them suitable for a diverse range of applications such as chemical sensors, flash memory and electro-optic devices[21-26]. Derivatives of PAni have also been used to form nanofibers, whereby monomers are first functionalised and then subsequently polymerised[27]. Sometimes however, this approach can adversely affect the polymerisation process due to steric effects[28].

Our approach is to covalently modify preformed PAni nanofibres, in a manner which essentially maintains the nano-morphology of the polymer material and leaves the unexposed Pani core unaffected. Covalent functionalisation of PAni has been reported previously

for the bulk material[8, 9, 28-30] with substituents such as sulphonic acid groups being added[8, 9, 29]. These can be introduced either through electrophilic or nucleophilic addition[28]. One such mechanism involves the use of fuming sulphuric acid[28]. However this approach is harsh, poses health and safety issues, and affects the form of the material (chain scission is a problem[9]). Attachment of sulfonic side-groups introduces self-doping to the PAni structure, and hence redox activity over a broader pH range[8, 9]. Weaker acid groups, such as mercaptoacetic acid, have also been attached and similarly result in a self-doped polymer[31]. As far as we are aware, post-synthesis functionalisation of PAni nanofibres (as opposed to bulk) has been reported only once before, by Epstein et al, who reported the reaction of sodium bisulphite ($Na_2S_2O_5$) with aligned PAni nanofibers to form sulfonated PAni [19]. Our technique differs from this approach in that it is template free and can be carried out in solution. Therefore, it can easily be scaled-up for the synthesis of bulk quantities.

We focus on the attachment of mercaptoundecanoic acid to the emeraldine base form of PAni (Scheme 1). In this case, previous literature[28] would suggest the thiol nucleophile should attach onto the electrophilic quinoid rings in the PAni backbone, as quinoimine units suffer nucleophilic attack with addition on the ring. Thiol attachment has previously been demonstrated for bulk PAni[28], but not for PAni nanofibres. We also show, for the first time, control over the level of side-chain attachment.

It is expected that a covalently bound COOH side-group should protonate the PAni backbone (with COO^- acting as the counter ion). Results obtained using a wide range of techniques including Fourier Transform Infra-Red, Thermal Gravimetric Ananlysis, Energy Dispersive X-ray Spectroscopy, UV-vis spectroscoscopy, conductivity measurements and electrochemistry are consitent with this self-doping behaviour.

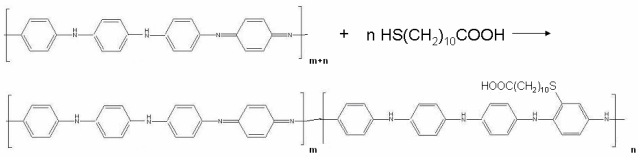

Scheme 1. Reaction scheme for the nucleophilic addition of mercaptoundecanoic acid (MA) to PAni. Substitution occurs onto the electrophilic quinoid ring with the elimination of hydrogen [28].

2. Experimental detail

Aniline (BDH), HCl (Fisher Scientific), ammonium peroxydisulfate (Aldrich), mercaptoundecanoic acid (Aldrich) and pH4 buffer (Fluka) were used. The aniline monomer was purified by vacuum distillation before use. Aniline is toxic and care must be taken during distillation. Purified aniline was stored under nitrogen in a sealed container at 4°C. Other chemicals were used as received.

Polyaniline nanofibres were synthesised under ambient conditions by interfacial polymerisation between an aqueous and an organic layer[11]. The aqueous layer contained 1M HCl as the dopant acid and ammonium peroxydisulfate (60 mmol, $(NH_4)_2S_2O_8$) as the oxidising agent. The organic layer contained purified aniline (200 mmol) dissolved in toluene. Green polyaniline appeared initially at the interface and then migrated into the aqueous phase, after 24 hours the reaction was complete. The product was purified by centrifugation (3000rpm/10min/3 cycles) and suspended as a colloid in deionised water.

PAni nanofibres were subsequently modified with mercaptoundecanoic acid (MA) by refluxing at 100°C for 2 hours in an aqueous pH 4 buffer. All experiments were carried out under identical conditions using 30ml of ~1.5mg/ml PAni aqueous dispersion. The amount of MA added was varied from 11mg (0.05 mmol) to 218mg (1 mmol). The product was purified by centrifugation (3000rpm/10min/3 cycles) and could be re-suspended as a colloid in deionised water.

Nanofibre morphology was studied using field emission scanning electron microscopy (FESEM) at an accelerating voltage of 20kV on a S-4300 Hitachi system. Samples were cast as films onto silicon wafers and coated with 10nm Au/Pd prior to imaging. Nanofibre diameters were measured from high-resolution FESEM images.

The bonding of MA side-chains to PAni nanofibres was investigated using a variety of techniques. Fourier transform infrared spectra (FTIR) were recorded in transmission mode from 400 to 4000cm^{-1}, for 100 repeat scans, with a resolution of 8cm^{-1} and at 1cm^{-1} intervals on a Perkin Elmer Spectrum GX FTIR. Samples were dried under vacuum at 50°C for 4 hours prior to FTIR and then mixed with dried KBr powder. Thermal Gravimetric Analysis (TGA) decomposition curves were obtained using a Mettler-Toledo TGA/SDTA851. Samples were heated from 25-700°C at 10°C/minute under nitrogen. Raman spectra were taken with an Avalon 785nm Raman Spectrometer at 2cm^{-1} resolution, 3sec per scan and 10-20 collections. A 785nm laser line was used as it can detect both doped and dedoped features in PAni. UV-vis spectroscopy was carried out on a Perkin Elmer UV-vis NIR Lambda 900 Spectrometer at 1nm resolution. Electrical surface conductivity (σ_s) was measured using a two-point probe technique. Colloid samples (in either a pH 2, or pH 9.2 medium) were filtered through Nylaflo 0.2μm filter paper. Filtered samples were then attached to a rigid insulating substrate, and contacts were made using silver paint and aluminum wires. The applied potential was increased at a rate of 0.05V/sec and the current flow in the circuit was measured accordingly. Values for σ_s were then calculated from $\sigma_s = G * s/l$, where G is the conductance of the circuit (measured from the slope of an I-V plot), s is the electrode seperation and l is the length of the electrodes

(Supporting Information S1) [32]. Electrochemistry of the fibres was investigated using a CH Instruments Electrochemical Analyser. Cyclic voltammetry results were obtained in 0.1M KCl electrolyte at pH 1, for a scan rate of 10mV/sec. A glassy carbon working electrode, a Pt wire counter-electrode and a Ag/AgCl reference electrode were used. Samples were drop cast onto a polished glassy carbon electrode, to form insoluble coatings after drying in air for several hours.

3. Results and Discussion

FESEM images show that homogenous PAni nanofibres are formed by interfacial polymerisation (Fig 1A-C). These fibres can be cast, from colloidal dispersions, as uniform films onto substrates such as silicon (inset Fig 1A). Fibre diameters measured using high-resolution FESEM images were found to be in the range 40-80nm (including a 10nm Au/Pd coating deposited for imaging purposes). After reflux, modified PAni-MA nanofibres were purified by centrifugation to remove by-products and any remaining unreacted species. By the third centrifugation, the supernatant becomes clear suggesting that all of the initial reactants have been removed. Centrifuged material can then be re-dispersed in solvents such as water to form colloid dispersions. As with PAni colloids, the solid phase settles gradually over time (depending on pH and concentration[17]) and can be re-distributed by shaking, making the material convenient to process. The quality of the dispersion decreases as the amount of MA used during the covalent attachment reactions was increased. After reacting with 218 mg (1mmol) MA the resultant PAni material could not be dispersed (even after 2 hours sonication).

FESEM images show that after reflux with MA, the fibre morphology remains essentially unaffected (Fig 1D). PAni-MA nanofibre diameters do not differ greatly from those measured for unmodified PAni (ranging

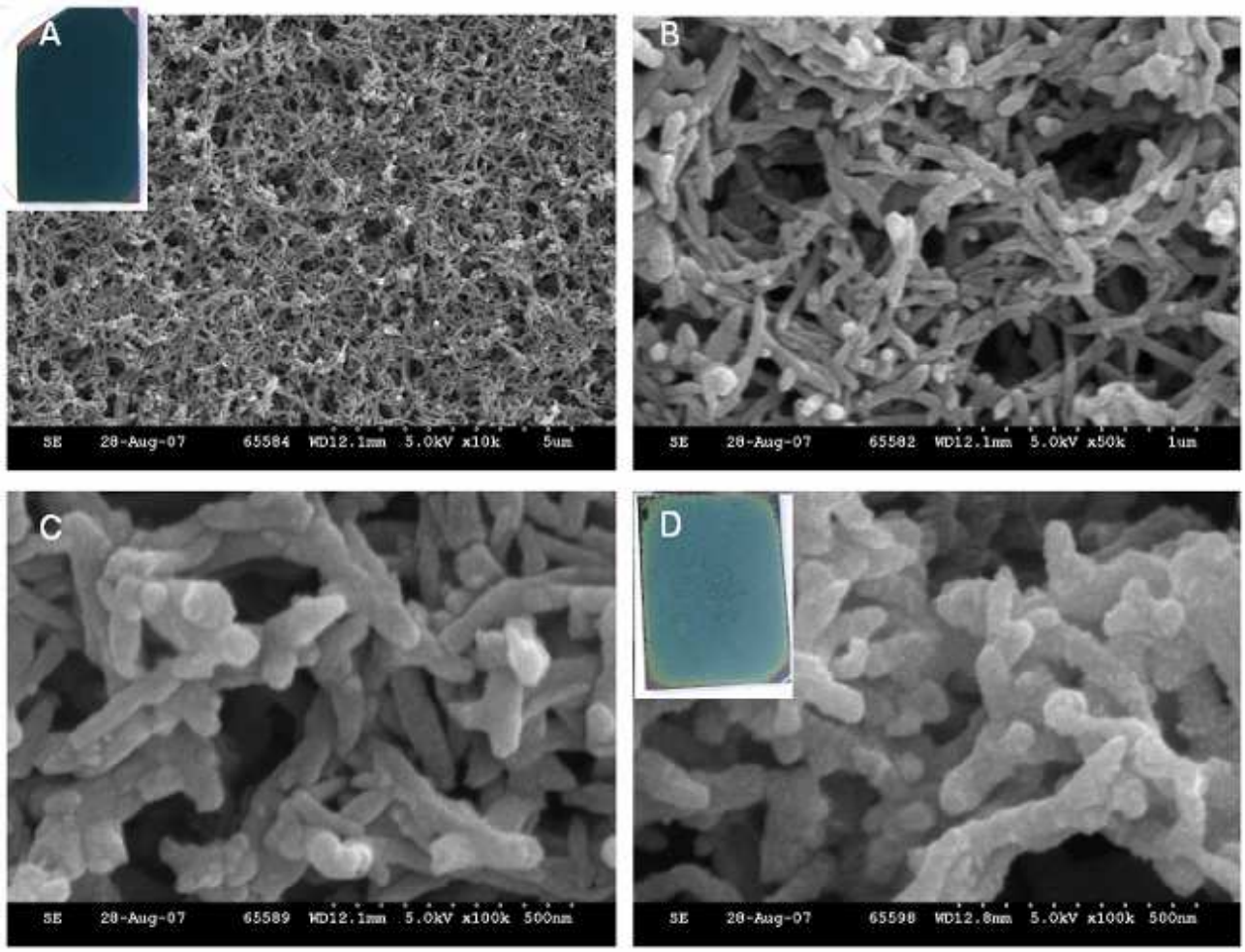

Figure 1: FESEM images A, B and C show PAni nanofibres. The surface roughness of nanofibres increases after reflux with MA (D) suggesting that functionalisation has occurred. Insets show optical images of homogenous films cast onto silicon substrates (2.5 x 1.5cm).

from 40-90 nm).

The morphology of the functionalised PAni-MA depends on the degree of side-chain attachment and FESEM images reveal that as the amount of MA-to-PAni was increased the nanostructure eventually degraded. Equal amounts of PAni (45mg) were functionalised with incremental amounts of 11, 22, 44, 55, 78, 109, 218 mg MA. For low levels of functionalisation, fibre nanomorphology is maintained. However above 44mg MA, small PAni fragments appear interspersed between the fibres (Supporting Information, S2). Initially only small amounts of the PAni fragments appear but this increases with the level of functionalisation, until for 218mg MA the nanofibre structure is lost altogether and only bulk PAni fragments are observed. This bulk material cannot be dispersed in water to form a colloid or deposited as a uniform film.

For the aniline:oxidant ratios used to synthesise the PAni precursor, the nanofibre yield scales linearly with volume at a rate of approximately 4mg/ml (this was measured for total reaction volumes in the range 40 to 400ml). Bulk quantities of these fibres could be refluxed simultaneously to form the functionalised material. The technique is therefore easily scalable.

Nanofibres were also characterised using Fourier Transform Infra-Red Spectroscopy (FTIR). For mercaptoundecanoic acid ($HS(CH_2)_{10}COOH$) a clean intense spectrum was obtained (Fig 2). From this spectrum a number of signature spectral features emerge. These include ν/cm^{-1} 1189, 1211, 1292, 1314, 1411, 1433, 2850 and 2918 (CH_2 twists, wags, in-plane bending and stretches[33, 34]), 686 (C-S[34]), a doublet at 723/730 (C-S[34]), 1105 (C-C stretch) and 1238 (C-C twist[35]), 1264(CH_2-S [36]), 465 (C-C=O [34]) and 1700 (C=O [33]).

These features appear alongside the typical PAni bands in a FTIR spectrum for functionalized PAni-MA fibres, thus suggesting that functionalisation has been achieved (Fig 2). Some transmission bands were slightly shifted indicating a change in the local chemical environment, consistent with covalently linked MA molecules. The C-S bond is interesting to consider as it occurs at the point of covalent bonding to the PAni backbone (Scheme 1). The C-S bond at 686cm^{-1} is downshifted by 3cm^{-1} for PAni-MA. Related doublet peaks at 723cm^{-1}/730cm^{-1} also shift to 720cm^{-1}/733cm^{-1} respectively, indicating a change in the C-S environment. The C-C alkyl stretch at 1105cm^{-1} shifts to 1107cm^{-1} for the functionalized material. Similarly CH_2, C-C and CH_2S bonds at 1211cm^{-1}, 1238cm^{-1} and 1264cm^{-1} shift to 1208cm^{-1}, 1233cm^{-1} and 1262cm^{-1} respectively (Fig 2). None of these shifts were observed when PAni and MA powders were mixed, rather than refluxed, together (Supporting Information, S3 and S4) confirming that these shifts are evidence of covalent bonding. The most intense peak is the C=O bond. This appears as a single peak at 1701±13cm^{-1} in MA powder and splits into a doublet at 1696cm^{-1}/1712cm^{-1} for PAni-MA. The splitting implies that two slightly different C=O environments exist and suggests some deprotonation of the hydrogen atom attached to the COOH acid group[33], consistent with self-doping. This splitting is not observed for low levels of MA attachment (11, 22mg) and becomes more noticeable as the amount of MA added during reflux is increased (218mg).

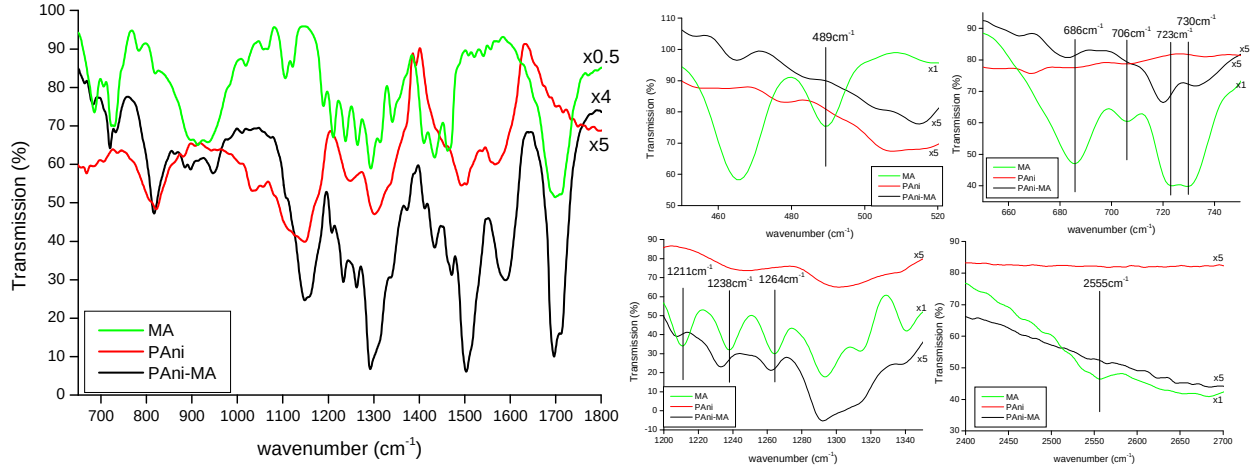

Figure 2: Characteristic MA peaks appear alongside PAni peaks in a FTIR spectrum for refluxed PAni nanofibres. Focusing on specific FTIR regions reveals that certain characteristic MA peak positions are shifted in PAni-MA. Also, bands at ν/cm^{-1} 489 (C-S-H), 706 (C-S-H) and 2555 (S-H) are absent for PAni-MA. (Spectra intensities have been magnified as indicated, spectra were also offset for clarity.)

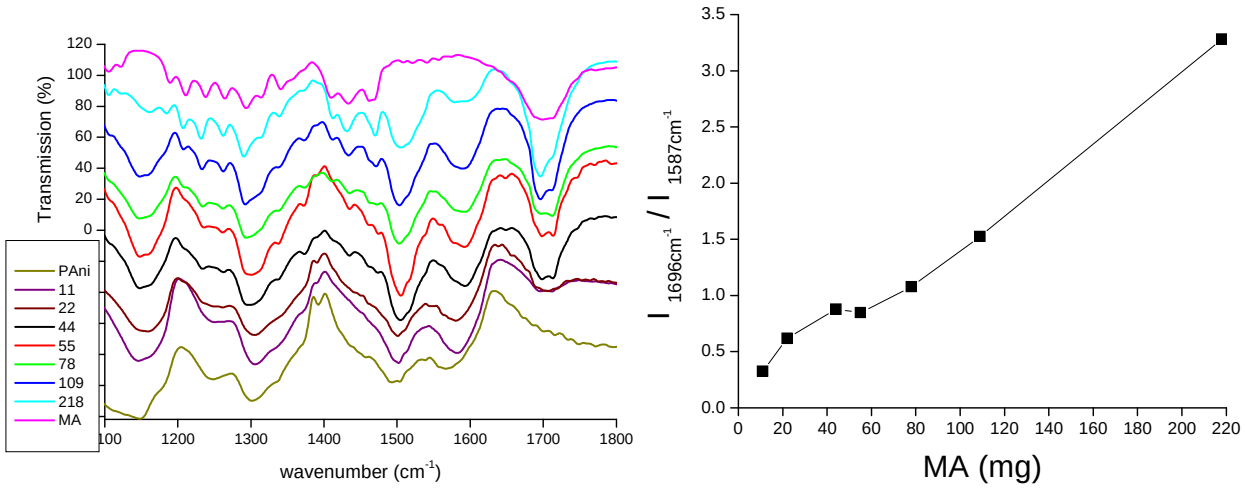

Figure 3. The intensity of characteristic MA peaks scale with the amount of MA added during reflux (inset, in mg), thus implying that the level of PAni functionalisation can be controlled. A plot of the band intensity at 1696 cm^{-1} to that at 1587 cm^{-1} shows an almost linear trend confirming that the level of functionalisation can be controlled by altering the amount of MA added during reflux.

The reaction shown in Scheme 1 proposes covalent attachment of the MA thiol bond to the PAni backbone. The S-H bond in MA appears at 489cm^{-1} and 706cm^{-1} (CSH out-of-plane bend and CSH in-plane bend respectively[37]). Another S-H stretch at 2556cm^{-1} is typically weak [34, 36, 37]. None of these bonds are present in PAni-MA spectra (Figure 2). They do however appear when PAni is mixed with MA powder (FTIR, Supporting Information). Their absence in PAni-MA spectra is further evidence of covalent attachment. From this we can deduce that covalent bonding of the MA thiol bond has occurred to the PAni backbone with the elimination of a hydrogen atom. FTIR spectra for different MA loadings (11, 22, 44, 55, 78, 109, 218 mg) show a clear trend in the band intensities (Fig 3). Band shifts are observed as before indicating covalent side-chain attachment for all degrees of functionalisation. A plot of the peak intensity at 1696cm^{-1} (due to C=O) compared with the intensity at 1587cm^{-1} (a characteristic PAni peak) shows an almost linear trend (Fig 3). Therefore we can say that the nanofibre functionalisation is scaling with the amount of MA added during reflux.

Thermal Gravimetric Analysis (TGA) revealed MA powder, unmodified PAni and PAni-MA to have very different decomposition profiles. Differentiating these TGA curves allows for a clearer interpretation of results (Fig 4). For MA the majority of decomposition occurs with a sharp peak at 230°C (90wt%). Unmodified PAni shows bulk decomposition between 300°C and 620°C (82wt% with a peak at 493°C), with weight loss at lower temperatures due to trapped solvent and other small molecules[38] (14wt% with a peak at 50°C and a further 4wt% at 233°C). By comparison, functionalised PAni-MA fibres show two significant areas of decomposition. One of these is centred at 495°C, which is consistent with a PAni component. A new feature appears similar in shape to the MA peak. For low levels of functionalisation (11mg and 22mg) this peak is centred at the same position as pure MA. However, as the degree of functionalisation increases, the position, and onset temperature, for this peak is up-shifted compared to that for MA. The onset of MA decomposition occurs at 120°C. The onset for PAni-MA occurs at 140°C for 11mg MA, and increases with the amount of MA added (Fig 4). This is consistent with greater entanglement and hydrogen bonding between polymer chains due to incremental amounts of covalently bound carboxylic acid side-chains. We therefore assign this peak to be a modified PAni-MA surface component.

The area of this PAni-MA decomposition peak scales with the amount of MA added during reflux thus confirming a clear trend in the level of functionalisation. That this modified surface volume scales with MA is consistent with FTIR results above. Also, it is interesting to note that no solvent peak appears in the PAni-MA plots, except for very low levels of MA ($\leq$ 22mg). Therefore, the amount of trapped solvent in PAni is decreasing as the level of carboxylate functionalisation increases (Supporting Information, S5). This appears to be linked to self-doping of the polymer by acid side-chains.

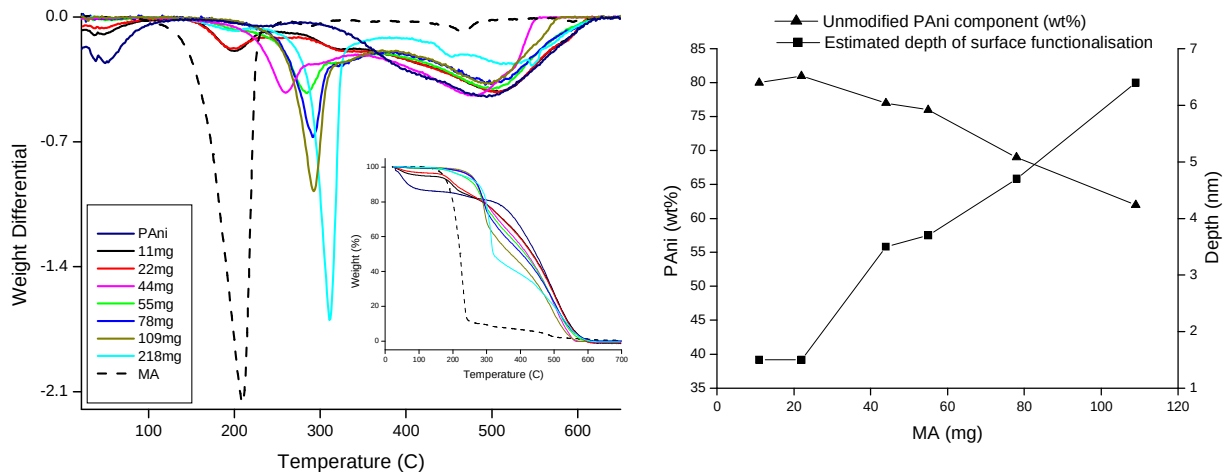

Figure 4. TGA plots (inset) of PAni, MA and PAni-MA. Derivatives are plotted for clearer interpretation. The decomposition of a functionalised PAni-MA component is seen as a sharp feature and the area of this peak scales with the amount of MA added (shown in mg) during reflux.

Approximating nanofibres to a cylinder of volume $\pi r^2 h$, allows us to estimate the depth of surface functionalisation. Assuming the density of PAni and PAni-MA to be equal, we tentatively suggest that the volume of functionalised PAni surface (approximated as a hollow cylinder of thickness $r-r_1$, where r_1 is the radius of the unmodified PAni core) as a percentage of the entire nanofibre (a cylinder of radius r) can be calculated using the area of the decomposition peak (area = $(r^2 - r_1^2) / r^2$). For a nanofibre radius (r) of 30 nm, consistent with the mid-range of values measured from FESEM images, the r_1 value ranges from approximately 28.5 nm to 23.6 nm. This suggests that the outermost 1.5 to 6.4 nm of the nanofibre is functionalised. This depth of surface functionalisation can be controlled by altering the amount of MA added during reflux (Fig 4).

Raman spectra of PAni and PAni-MA show similar spectral changes in response to the local chemical environment (Fig 5). For low pH values the polymer exists in the doped, conductive state. Increasing the pH causes a change in the bonding structure of the material. Signature bands between 1300-1400 cm^{-1} appear for the doped material. These are less significant at higher pH values, and strong bands between 1400-1500 cm^{-1} reflect the dedoped state. In particular, peaks at 1340cm^{-1} can be assigned to a $C\text{-}N^{\bullet+}$ polaron stretch[39, 40] and peaks at 1480cm^{-1} are characteristic of C=N quinoid groups[40]. Raman evidence therefore indicates that the redox state of PAni can still be switched post-functionalisation. This switching is accompanied by an obvious colour change in the material, from green to purple upon dedoping, and can be further studied using UV-vis spectroscopy.

UV-vis spectra for PAni are sensitive to the conjugation and conformation of aniline rings. PAni and PAni-MA show similar spectral changes as a response to doping and de-doping (Fig 6). In a low pH environment, a characteristic PAni band appears at 412nm and represents the doped state. The tail above 600nm can be attributed to a polaron transition[41]. These bands are also observed for the functionalised material (22mg and 44mg MA). Another band also appears at 344nm for PAni-MA. This band is characteristic of a $\pi\text{-}\pi^*$ transition. It is absent in fully doped PAni but expected for the functionalised material, due to quinoid ring substitution. The intensity of this peak at 344nm increases with functionalisation (Fig 6).

When PAni fibres are exposed to a higher pH environment, a $\pi\text{-}\pi^*$ transition band at 341nm dominates due to dedoping. For unmodified PAni, the peak at 412nm disappears completely. This corresponds to a dramatic decrease in conductivity. For the modified PAni-MA, this peak is still present and it's intensity scales with the level of functionalisation (Fig 6).

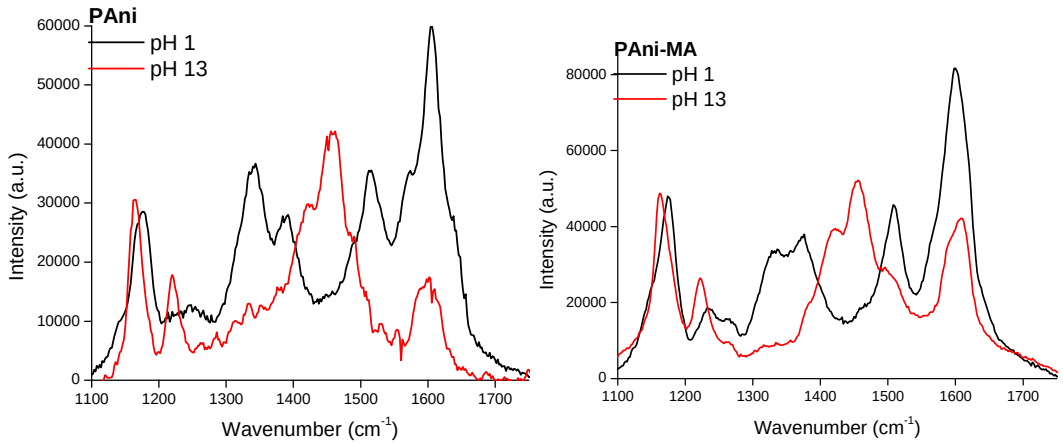

Figure 5. Raman spectra of PAni and PAni-MA reflect similar changes in molecular structure as a response to pH. (Spectra have been normalised.)

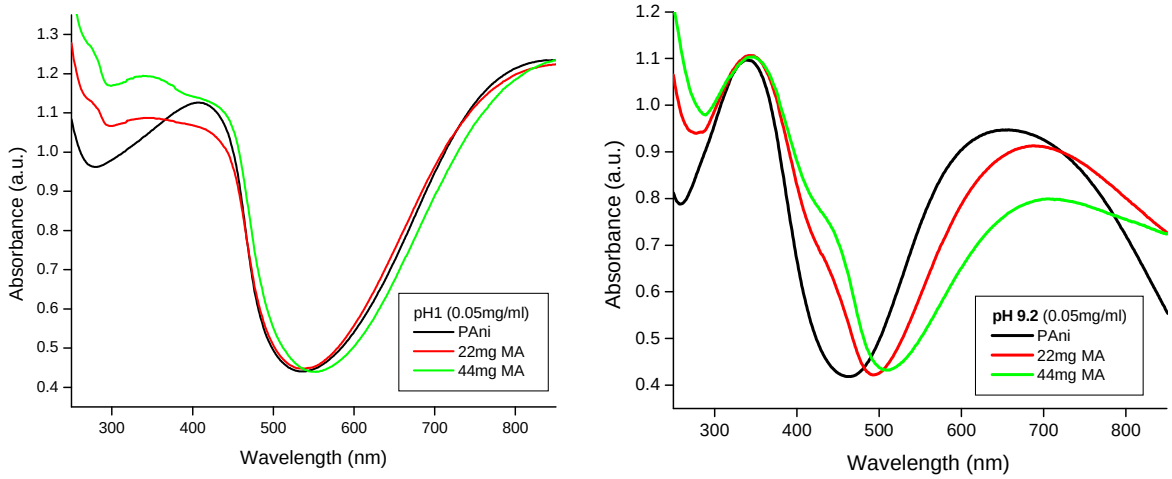

Figure 6. UV-vis spectra differ slightly for PAni and PAni-MA. Redox switching is accompanied by a change in colour from green to purple, in both materials, as the pH increases. (Spectra have been normalised.)

A peak at 655nm can be assigned to the quinoid fraction of the PAni backbone. This peak shows a bathochromic shift as the degree of functionalisation is increased (λ = 655, 688, 705nm for samples prepared using 0, 22 and 44mg MA). This is consistent with a change in local pH, which can be attributed to the presence of carboxylic acid side-groups, and similar peak shifts have been reported for PAni when dispersed in solvents of increasing polarity[42].

The degree of oxidation can be estimated from the ratio of the 655nm to the 344nm band[42]. Ratios are 0.86 to 0.82 and 0.72, for 0mg, 22mg and 44mg MA. This is consistent with an increase in the quinoid fraction and implies an increase in the oxidation state of PAni-MA compared to PAni. A slight bathochromic shift is also observed where the peak at 341nm shifts to 346nm, consistent with ring substitution[43]. At pH 9.2, the polaron tail above 600nm does not completely diappear for PAni-MA, unlike for PAni. Therefore, functionalised fibres maintain some conductive characteristics which are absent for unmodifed PAni in higher pH environments. This observation is consistent with conductivity measurements.

Surface conductivity values were measured for fibres at pH 2 (HCl) and pH 9.2 (buffer). The surface conductivity for unmodified PAni nanofibres switched from 1.47×10^{-3} S/□ to 2.85×10^{-7} S/□ in response to dedoping. For the modified fibres the conductivity of the doped fibres was lower than that for PAni, and was

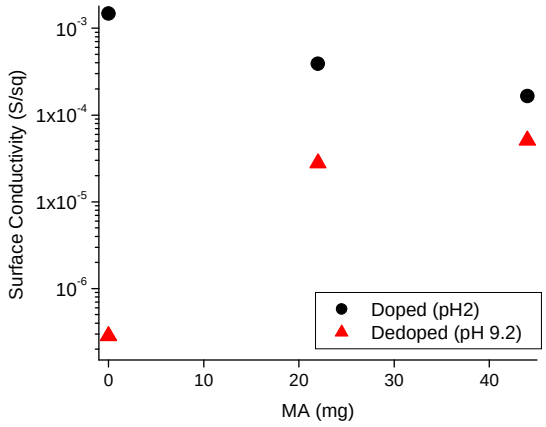

Figure 7. Conductivity measurements show greater stability as the degree of functionalisation increases.

calculated to be $3.9x10^{-4}$ S/□ for the sample prepared using 22mg MA. This can be explained as a decrease in the effective π-conjugation length of the polymer due to increased substitution. The switch in conductivity upon dedoping however, was less dramatic and switched to $2.8x10^{-5}$ S/□. For 44mg MA conductvity switched from $1.65x10^{-4}$ S/□ to $5.1x10^{-5}$ S/□ upon dedoping. This reflects greater stability in electrical conductivity for the functionalised nanomaterial.

Functionalisation of PAni nanofibres also affects the electrochemical properties of the material. PAni is an electrochemically active material which can switch between three states (leucoemeraldine, emeraldine and pernigraniline). Each redox state varies in the number of amine versus imine groups present along the polymer backbone, and this determines polymer properties such as conductivity and colour. Cyclic voltammetry (CV) shows that, as expected, unmodified PAni nanofibres switch between three states under acidic conditions (Figure 8), and this switching is fully reversible for repeated redox cycling. For PAni nanofibres, a double reduction peak is observed between 0.7V and 0.4V. This has been observed (though not explained) previously [44], and appears to be a characteristic of the nanofibre form of PAni (rather than bulk PAni). We suggest that it is due to the higher surface area of Pani in it's nanoform. The sharpness of the peak suggests that it is a surface phenomena, and it may be that there is a distinct surface response as well as a bulk PAni response. It is strange however that this should only occur on one redox couple. Previously it has been reported that the doublet becomes a single peak after repeated cycling or prolonged dispersion of the aqueous colloids[44]. This may be accompanied by a degredation of the nanoform, and requires further investigation.

The electrochemical behaviour of polyaniline nanofibres when modified with MA, is altered due to the presence of covalently bound acid functionalities along the polymer backbone. An additional redox peak appears between 02.V and 0.4V. Similar behaviour has been

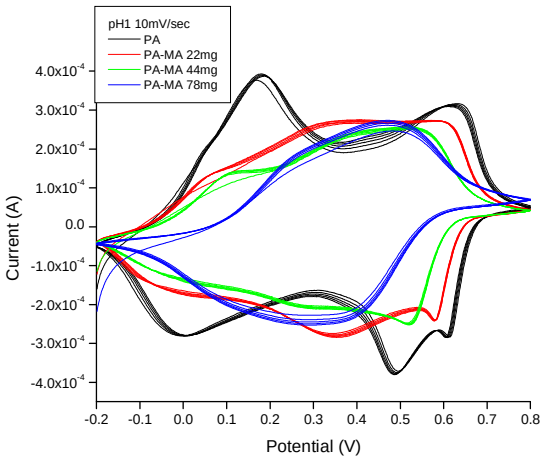

Figure 8. Cyclic voltammetry of PAni nanofibres was compared with that for the functionalised material. As the level of functionalisation increases, only one redox peak appears.

reported previously for a polyaniline composite formed combining PAni with poly(2-methoxyaniline-5-sulfonic acid), where the appearance of an additional redox peak was attributed to the interconversion of emeraldine and pernigraniline for the non-Pani component.[45] Here we can attribute the additional peak to the interconversion of PAni-MA between two states. As the amount of MA added to PAni increases, the number of unfunctionalised quinoid rings (hence imine sites) along the PAni backbone decreases. For low levels of MA functionalisation, redox behaviour is similar to that of PAni. However, as MA increases (and covalently bound COO^- becomes the dominant dopant), CV scans show only one peak rather than the two observed for PAni (Figure 8). This indicates switching between two, rather than three redox states. This observation supports the claim that where small amounts of MA are attached, both external acid groups and covalently bound acid groups act as dopants. Redox cycling is reversible for both PAni and PAni-MA, and current flow for both oxidation and reduction is approximately equal.

Trapped solvent in unmodified PAni is mainly due to the presence of dopant ions (Cl^- in our case). EDXS for PAni show an intense chlorine peak as expected (Figure 9). A sulphur peak also appears which is only slightly less intense than the Cl peak, and more intense than the carbon peak (due to the relatively low atomic mass of carbon). A low intensity oxygen peak was also detected. This suggests that sulphate ions may also be present as dopant (presumably a by-product from the oxidant $(NH_4)_2S_2O_8$ used during aniline polymerisation). Closer examination of FTIR spectra for PAni reveals peaks at $619cm^{-1}$ and $1033cm^{-1}$ which are consistent with a sulfonate S=O stretch (Supporting Information, S6).[9] TGA also shows a decomposition peak at 233°C (4wt%) for PAni, which is consistent with SO_3^{2-} dopant.

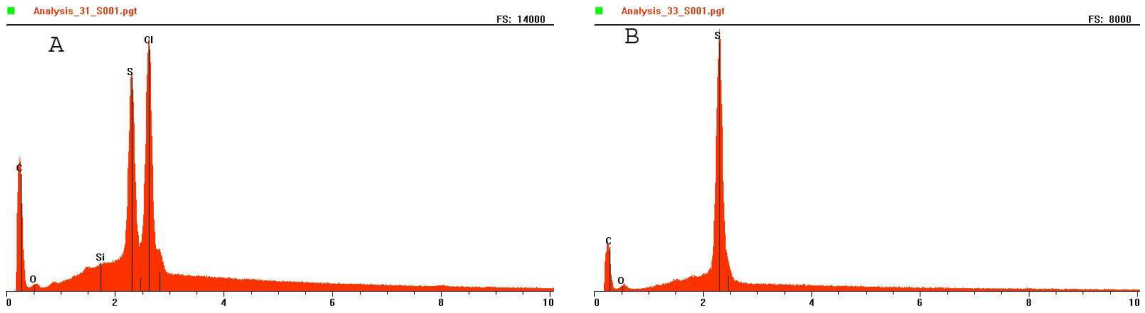

Figure 9. EDXS spectra show that chlorine is present in doped PAni (A) but absent in the functionalised PAni-MA (105mg) material (B). Therefore it cannot be acting as a dopant. HCl appears to be the dominant dopant in PAni, but SO_4^{2-} is also significant.

EDXS spectra for the functionalised PAni-MA show an intense sulphur peak. FTIR spectra however, show no S=O peaks for PAni-MA (Supporting Information, S6). Therefore, we attribute this to the thiol group of the MA side-chains (low intensity carbon and oxygen peaks are also present). The Cl peak is missing for PAni-MA indicating an absence of external dopant. This evidence suggests the neither sulphate nor chloride ions are present as dopants in the functionalised nanofibres. Combining evidence from FTIR, TGA and EDXS we suggest that for sufficient levels of functionalisation COO^- replaces external dopants (SO_3^{2-} and Cl^-). Therefore, we suggest that PAni-MA becomes a self-doped material.

This claim is further supported by surface conductivity measurements at pH 9, where values were two orders of magnitude greater for PAni-MA (22mg) than for unmodified PAni.

4. Conclusions

We have demonstrated the successful functionalisation of solution based PAni nanofibres. We have also shown, for the first time, control over the extent of side-chain attachment to these one-dimensional nanostructures. Functionalisation can be controlled using a simple, scalable and inexpensive technique. The modified nanofibres maintain their ability to switch between diffferent forms displaying distinctly different optical properties (as shown by Raman and UV-vis spectroscopy), thus making them suitable for adaptive sensing applications. Acid terminated chains can be used to introduce self-doping behaviour, hence reducing the need for an external dopant. The attachment of carboxylated functional groups to polyaniline nanofibres provides a route for manipulating the surface chemistry of nanofibres. While interesting materials in themselves, these functionalised nanofibres are also attractive as molecular scaffolds for building yet more innovative derivatives that nonetheless retain the basic underlying nanostructure and intrinsic characteristics of PAni. That we have demonstrated the ability to regulate the extent of side-chain attachment to one-dimensional objects, in a safe and simple manner, represents a step forward in the area of adaptive nano-structured materials.

Acknowledgements

The authors acknowledge funding from Science Foundation Ireland under the 'Adaptive Information Cluster' award no. SFI 03/IN.3/1361. Prof. Gordon G. Wallace thanks the Australian Research Council for on-going support. The authors also thank Dr. Steven Bell (Queen's University Belfast) for helpful discussions.

References

[1] S. C. A. Drury, M. Kroll, V. Nicolosi, N. Chaure, W.J. Blau, , Chemistry of Materials 19 (2007) 4252.

[2] W. Belzig, Nat. Nanotechnol. 1 (2006) 167-168.

[3] J. M. Bao, M. A. Zimmler, F. Capasso, X. W. Wang, Z. F. Ren, Nano Lett. 6 (2006) 1719-1722.

[4] Nikoobakht, Chemistry of Materials 19 (2007) 5279.

[5] M. M. S. L. Ci, X. Li, R. Vajtai, P.M. Ajayan, Adv Mater 19 (2007) 3300.

[6] R. Blake, Y. K. Gun'ko, J. Coleman, M. Cadek, A. Fonseca, J. B. Nagy, W. J. Blau, J. Am. Chem. Soc. 126 (2004) 10226-10227.

[7] Y. Cui, Q. Q. Wei, H. K. Park, C. M. Lieber, Science 293 (2001) 1289-1292.

[8] A. J. E. Jiang Yue, J. Am. Chem. Soc. 112 (1990) 2800-2801.

[9] H. Salavagione, G. M. Morales, M. C. Miras, C. Barbero, Acta Polymerica 50 (1999) 40-44.

[10] C. O. Baker, B. Shedd, P. C. Innis, P. G. Whitten, G. M. Spinks, G. G. Wallace, R. B. Kaner, Adv Mater 20 (2008) 155-+.

[11] W. R. Small, F. Masdarolomoor, G. G. Wallace, M. Panhuis, J Mater Chem 17 (2007) 4359-4361.

[12] J. G. Roh, H. R. Hwang, J. B. Yu, J. O. Lim, J. S. Huh, Journal of Macromolecular Science-Pure and Applied Chemistry A39 (2002) 1095-1105.

[13] R. Byrne, D. Diamond, Nat. Mater. 5 (2006) 421-424.

[14] A. G. MacDiarmid, Synthetic Metals 84 (1997) 27.

[15] N. R. Chiou, A. J. Epstein, Synthetic Metals 153 (2005) 69-72.

[16] J. X. Huang, R. B. Kaner, Chemical Communications (2006) 367-376.

[17] D. Li, R. B. Kaner, Chemical Communications (2005) 3286-3288.

[18] D. Li, R. B. Kaner, J Mater Chem 17 (2007) 2279-2282.

[19] N. R. Chiou, C. M. Lui, J. J. Guan, L. J. Lee, A. J. Epstein, Nat. Nanotechnol. 2 (2007) 354-357.

[20] F. Masdarolomoor, P. C. Innis, S. Ashraf, R. B. Kaner, G. G. Wallace, Macromol. Rapid Commun. 27 (2006) 1995-2000.

[21] S. Virji, J. X. Huang, R. B. Kaner, B. H. Weiller, Nano Lett. 4 (2004) 491-496.

[22] S. Virji, R. B. Kaner, B. H. Weiller, J. Phys. Chem. B 110 (2006) 22266-22270.

[23] S. Virji, R. B. Kaner, B. H. Weiller, Chemistry of Materials 17 (2005) 1256-1260.

[24] S. Virji, J. D. Fowler, C. O. Baker, J. X. Huang, R. B. Kaner, B. H. Weiller, Small 1 (2005) 624-627.

[25] R. J. Tseng, J. X. Huang, J. Ouyang, R. B. Kaner, Y. Yang, Nano Lett. 5 (2005) 1077-1080.

[26] J. X. Huang, S. Virji, B. H. Weiller, R. B. Kaner, J. Am. Chem. Soc. 125 (2003) 314-315.

[27] H. D. Tran, R. B. Kaner, Chemical Communications (2006) 3915-3917.

[28] D. F. Acevedo, H. J. Salavagione, M. C. Miras, C. A. Barbero, J. Braz. Chem. Soc. 16 (2005) 259-269.

[29] C. Barbero, G. M. Morales, D. Grumelli, G. Planes, H. Salavagione, C. R. Marengo, M. C. Miras, Synthetic Metals 101 (1999) 694-695.

[30] D. F. Acevedo, J. Balach, C. R. Rivarola, M. C. Miras, C. A. Barbero, Faraday Discuss. 131 (2006) 235-252.

[31] C. C. Han, R. C. Jeng, Chemical Communications (1997) 553-554.

[32] E. Lahiff, R. Leahy, J. N. Coleman, W. J. Blau, Carbon 44 (2006) 1525-1529.

[33] N. Goutev, M. Futamata, Appl. Spectrosc. 57 (2003) 506-513.

[34] J. L. Castro, M. R. Lopez-Ramirez, J. F. Arenas, J. C. Otero, J. Raman Spectrosc. 35 (2004) 997-1000.

[35] A. M. P. Hussain, A. Kumar, Bull. Mater. Sci. 26 (2003) 329-334.

[36] K. Moller, J. Kobler, T. Bein, J Mater Chem 17 (2007) 624-631.

[37] V. Krishnakumar, R. J. Xavier, Spectrochimica Acta Part a-Molecular and Biomolecular Spectroscopy 60 (2004) 709-714.

[38] K. Luo, N. L. Shi, C. Sun, Polym. Degrad. Stab. 91 (2006) 2660-2664.

[39] R. Mazeikiene, A. Statino, Z. Kuodis, G. Niaura, A. Malinauskas, Electrochem. Commun. 8 (2006) 1082-1086.

[40] C. Liu, J. X. Zhang, G. Q. Shi, F. E. Chen, J. Appl. Polym. Sci. 92 (2004) 171-177.

[41] C. Barbero, M. C. Miras, B. Schnyder, O. Haas, R. Kotz, J Mater Chem 4 (1994) 1775-1783.

[42] T. Yasuda, I. Yamaguchi, T. Yamamoto, J Mater Chem 13 (2003) 2138-2144.

[43] M. Inoue, F. Medrano, M. Nakamura, M. B. Inoue, Q. Fernando, J Mater Chem 4 (1994) 1811-1814.

[44] T. Z. Xingwei Li, Gengchao Wang, Yunpu Zhao, Mater. Lett. 62 (2008) 1431–1434.

[45] F. Masdarolomoor, P. C. Innis, S. Ashraf, G. G. Wallace, Synthetic Metals 153 (2005) 181-184.